48TH TURBOMACHINERY & 35TH PUMP SYMPOSIA
HOUSTON, TEXAS | SEPTEMBER 9-12, 2019
GEORGE R. BROWN CONVENTION CENTER

ADDRESSING HIGH SUB-SYNCHRONOUS VIBRATIONS IN A TURBOEXPANDER EQUIPPED WITH ACTIVE MAGNETIC BEARINGS

Tadeh Avetian, P.E.
Director of Engineering
L.A. Turbine
Valencia, CA, USA

Junyoung Park, Ph.D
Machinery Engineer
Samsung Engineering CO. Ltd.
Seoul, South Korea

Luis E. Rodríguez.
Design Engineer
L.A. Turbine
Valencia, CA, USA

Tadeh Avetian is currently Director of Engineering at L.A. Turbine in Valencia, California, where he is responsible for identifying and defining research and development projects and directing turboexpander design for new and aftermarket equipment. Mr. Avetian first joined L.A. Turbine in 2011 as Core Design Manager. His responsibilities included designing all new and custom turboexpanders and supporting the design of auxiliary systems. Mr. Avetian previously held the position of Rotating Machinery Engineer at Technip USA, Inc. (now TechnipFMC). In this role, he specified, sourced and evaluated equipment for the construction of hydrocarbon processing plants, refineries and petrochemical facilities. Mr. Avetian is a California-registered Professional Engineer (P.E.) with a Bachelor and Master of Science in Mechanical Engineering from California State Polytechnic University, Pomona, California.

Luis E. Rodríguez is a Design Engineer with L.A. Turbine in Valencia, California, where he is responsible for the mechanical design of turboexpanders. Previously, he served for 10 years in the engineering department of Sulzer Turbo Services (now Sulzer Rotating Equipment Services) in La Porte, Texas. He has co-authored papers published in the ASME Journal of Tribology and the STLE transactions. He holds a B.S. degree from Universidad Simón Bolívar in Venezuela (2001), and a M.S. from Texas A&M University in College Station, Texas (2004). He is a licensed Professional Engineer in the State of Texas since 2007 (currently inactive).

Junyoung Park, Ph.D is the Rotating Machinery Leader Engineer at SAMSUNG ENGINEERING Co. Ltd. Since joining the company in 2008, his responsibilities include detail engineering of rotating machinery and trouble shooting of mechanical vibration issues, mainly in Oil & Gas and Petrochemical Plants. He is involved in several on-going projects working with rotating machinery, such as pumps, compressors, turbines and expander-compressors. Dr. Park received his M.S degree (Mechanical Engineering, 2002) from University of Southern California and Ph.D degree (Mechanical Engineering, 2008) from Texas A&M University.
During his Ph.D period, he worked with several research projects sponsored by NASA. He is a member of KCIMD (Korea Certification Institute for Machine Diagnostics)

ABSTRACT

It is well known that cross-coupled forces can be induced by aerodynamic interactions between rotating and stationary components in a turbomachine. There is an abundance of well-documented case studies addressing unstable sub-synchronous vibration on process compressors in the technical literature. The API-617 standard addresses this topic in its rotordynamics section, requiring OEM designers perform Level 1/2 stability analyses to ensure stable designs. Potential destabilizing impeller aerodynamic forces must be considered in these analyses, utilizing equations such as the API-Wachel equation. Other analytical tools are also necessary to predict cross-coupled forces from components such as labyrinth seals. Broadly speaking, such approaches have proven to be sufficient for the design of centrifugal and axial compressors. However, the experience of the authors exposes the fact that rotordynamic instabilities induced by cross-coupling in radial inflow turbine applications are less well understood.

Accounts of such problems in turboexpanders are scant in the technical literature. In the past, various explanations have been offered to explain excessive sub-synchronous vibrations in turboexpanders. In one instance that involved a turboexpander equipped with a magnetic bearing, it was suggested that liquids in the expander inlet was the root cause (Shokraneh, 2016). In another published case study, a similar sub-synchronous vibration was induced by rotordynamic instabilities likely due to aerodynamic cross-coupling, on a machine operated with oil bearings and dry process gas throughout the flow path (Lillard, 2017). While operational problems with turboexpanders with oil bearings or magnetic bearings are rare, further understanding of the cross-coupled characteristics is necessary.

This paper presents the experience of the authors with a turboexpander (TEX) equipped with active magnetic bearings (AMBs) in a natural gas processing facility. The TEX was unable to achieve design performance due to high sub-synchronous vibration since its commissioning. Rotordynamic simulations revealed that the most likely root-cause of the high vibration was the excitation of an unstable rigid body mode of the rotor-bearing system due to high cross-coupled stiffness effects. This paper also contains a summary of the redesign features incorporated in the TEX that resolved the sub-synchronous vibration.

INTRODUCTION

Turboexpanders

Turboexpanders are standard in the natural gas industry for liquefaction and dew point control. They are also used in the petrochemical, air separation, refrigeration and power generation industries. Figure 1 shows a cross-section of a typical TEX design. The expansion stage consists of a radial inflow turbine, often with variable-position inlet guide vanes. The compression stage is comprised of a centrifugal compressor stage with a vaneless diffuser. The latest revision of API-617 addresses TEX design in Chapter 4, with AMB requirements covered in Chapter 1, Annex E.

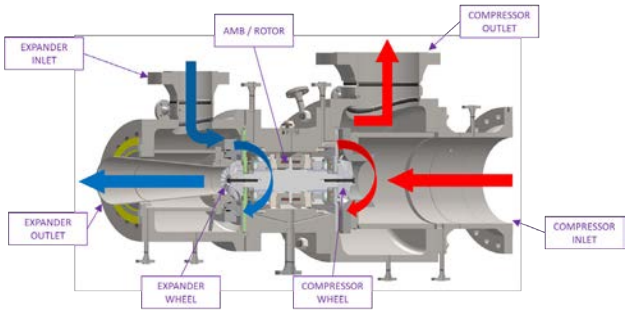

Figure 1. Typical TEX design equipped with AMBs.

Figure 2 depicts the flow diagram of the gas plant where the subject TEX was installed. Note that the inlet to the TEX is usually downstream of a gas-liquid separator, implying the expander inlet gas is saturated. In addition, most natural gas processes deal with hydrocarbon compositions that have a retrograde dew point. Figure 3 shows the phase diagram of such a composition, indicating the thermodynamic state of the TEX inlet. The retrograde dew point is a point on the vapor-liquid equilibrium line in a phase diagram in which a decrease in temperature *or* pressure results in condensing of the gas, ultimately leading to liquids entering the TEX. This is unlike the more familiar normal dew point, in which a saturated liquid will vaporize on decreasing pressure at constant temperature.

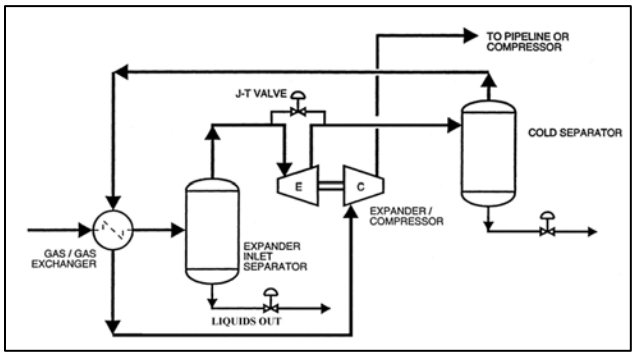

Figure 2. Typical natural gas liquefaction process.

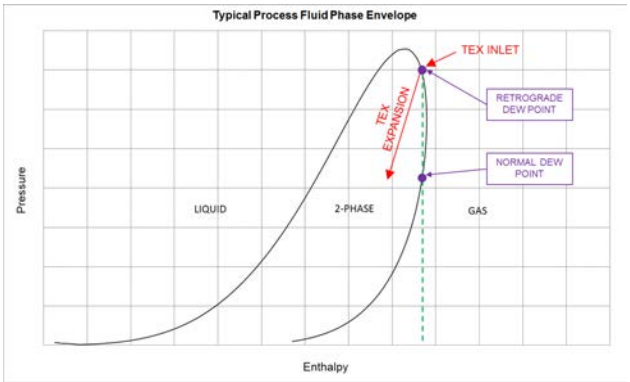

Figure 3. Typical natural gas phase diagram.

In a TEX, the inlet gas is accelerated through the stator, or inlet guide vanes, leading to very high swirl, or tangential velocity. This swirling gas then enters the expander wheel, which is ideally spinning fast enough such that its blade tip speed matches the gas swirl velocity, leading to low incidence. This occurs closest to the design point of the TEX, with higher incidence occurring in very low flow operating cases. The gas performs work absorbed by a loading device (e.g. a compressor), and as a result loses angular momentum as it travels through the expander wheel. This power balance occurs at a certain speed, based on the design and sizing of the expander and compressor wheels. Jumonville, 2010, presents a comprehensive tutorial on turboexpanders.

The typical TEX is designed as a 50% reaction turbine. This means that half of the static enthalpy change occurs across the stator, or inlet guide vanes, and the other half across the rotor, or expander wheel. Referring again to Figure 3, the implication is that liquids will be formed as the gas flows through the guide vanes. This means that in a typical TEX, the expander wheel has high velocity, two-phase fluid surrounding its outer diameter. The aerodynamic forces imparted on the rotor due to this complex two-phase flow are not well understood, particularly regarding their effects on lateral rotordynamics.

ACCOUNT OF THE VIBRATION PROBLEM

The original TEX was designed for the performance requirements listed in Table 1. In so far as power and speed are concerned, these operating parameters are typical for a natural gas application of a TEX, including AMB applications. Both the OEM and the AMB supplier had positive experiences with units of similar performance requirements.

The design of the expander stage was similar to the cross-section depicted in Figure 4. It was composed of four inlet guide vanes directing flow to a 14-bladed, shrouded (closed), aluminum wheel. The wheel seals were a tapered labyrinth type, both on the front and back of the wheel, with the teeth on the wheel. The shaft seal was a single port labyrinth seal, also typical of a TEX.

Table 1. Design Performance Conditions.

	Expander	Compressor
MW [lb/lbmol]	23.82	20.82
Pin [psia]	1165	247
Tin [F]	86	99
Mass Flow [lb/hr]	160,000	121,000
Pout [psia]	286	450
Tout [F]	-9	195
Speed [rpm]	30,000	30,000
Diameter [in]	7.5	10
Efficiency	86%	77%
Power [HP]	2200	
Torque [lb-ft]	385	

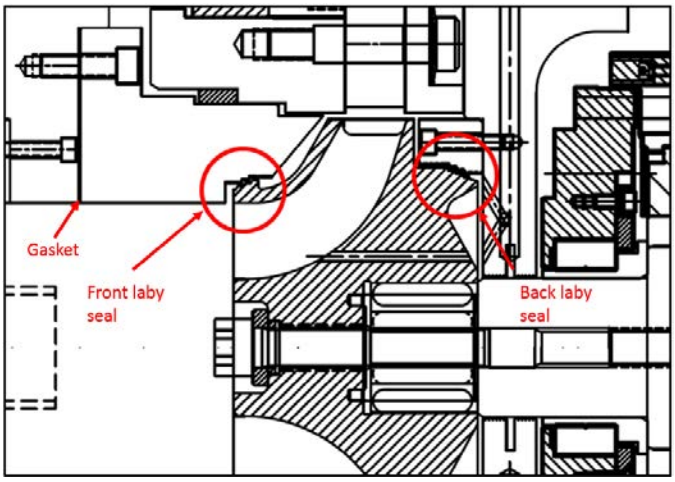

Figure 4. Typical expander cross-section indicating front and back labyrinth seals.

Early Commissioning Efforts – July-August 2017

Initial startup efforts began in late July of 2017. The machine was unable to reach design speed because it suffered two trips on high sub-synchronous vibration at a speed around 15,000 rpm. The amplitude of vibration on the expander side bearing reached 3-4 mils, above the shutdown threshold of 3 mils (see Figure 5). The frequency of vibration was approximately 40-50 percent of the rotation speed. Table 2 and Figure 6 detail the initial startup attempts.

Table 2. Log of initial startup attempts.

2017	07/30	07/31	08/01	08/21	08/31
Speed (Hz)	244	244	241	276	348
Vibration (Hz)	100	111	90.9	137	175
Speed Ratio	0.410	0.455	0.377	0.496	0.503

Note: Speed is expressed in Hz (rpm/60) to compare to vibration frequency.

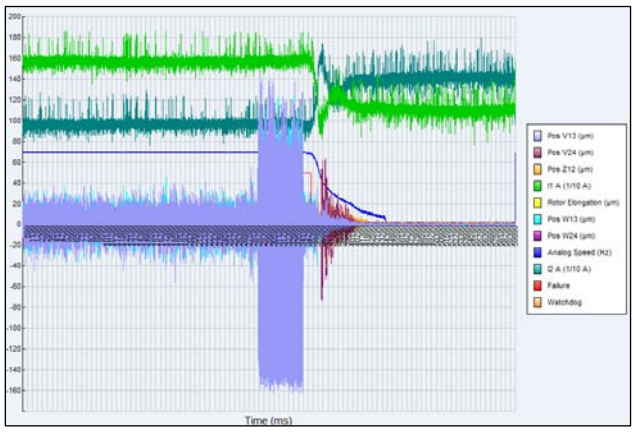

Figure 5. Sample time history of high sub-synchronous vibration trips.

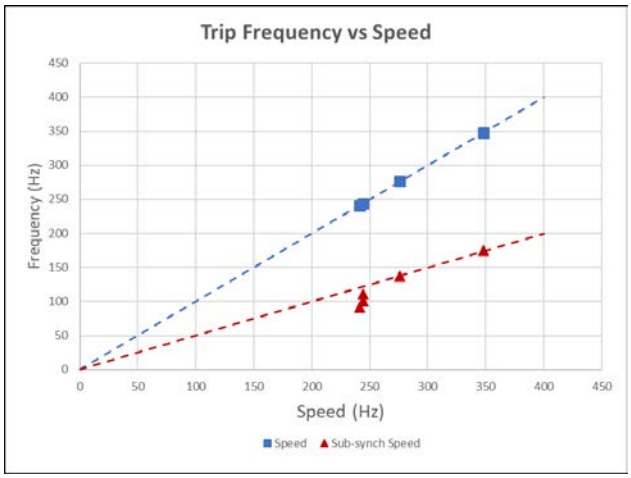

Figure 6. Plot of initial startup attempts.

This behavior was very similar to the OEM's experience with another TEX in 2013, henceforth known as the N'Kossa Project (Shokraneh, 2016). Based on the N'Kossa experience, the OEM, AMB supplier and EPC/End User suspected that liquid presence around the wheel and the front labyrinth seals was the root cause of rotordynamic instability. This became the initial working hypothesis in this project, which led to focus the efforts to ensuring that the inlet to the TEX was dry. It also led to questioning whether a shrouded expander wheel had been the most appropriate design.

The actual process conditions deviated from design, though not substantially. The expander operated at a higher discharge pressure than design (435 psia vs. 286 psia). The compressor operated with a higher suction pressure than design (435 psia vs. 247 psia). Considering the liquid presence as a root cause, it was hypothesized that the high discharge pressure of the expander was not leading to enough of a pressure difference across the wheel labyrinth seals, leading to liquid build-up.

In addition, the gas composition and molecular weight of the expander inlet stream proved difficult to quantify. The EPC and End User made extensive efforts to determine the actual gas composition, however continuous testing from various sample points revealed a significant uncertainty (see Figure 7).

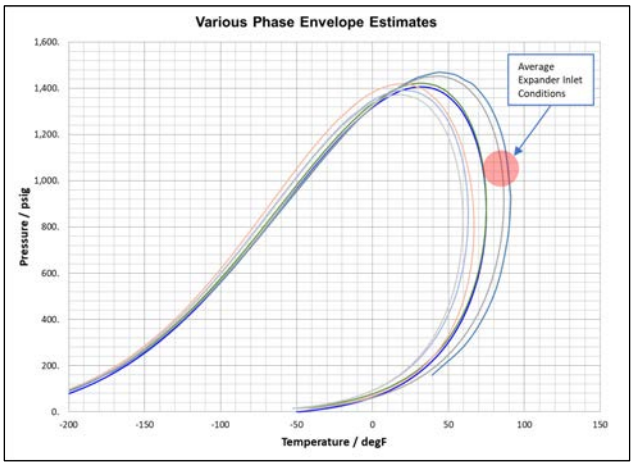

Figure 7. Various phase envelope estimates from gas analysis.

It was also observed that there was an insufficient supply of seal gas pressure which led to a negative differential pressure across the expander shaft seal. Operators were forced to bypass the shut-down control in order to continue commissioning. It was feared, at first, that process gas leaking through the expander shaft seal into the bearing housing may also have contributed to vibration problems. It was later confirmed that this negative differential was not a root cause because higher pressure seal gas was eventually supplied, yet the sub-synchronous vibration issues persisted.

An attempt was made to operate the machine with the IGVs in almost fully open position, using the expander inlet valve to attempt to regulate flow. The expectation was that fully opening the IGVs would reduce the amount of liquids present around the wheel outer diameter (OD), as well as the swirl velocity. However, the machine shut down again due to high sub-synchronous vibration.

Subsequent Troubleshooting Efforts – August-September 2017

The machine was taken offline and removed for disassembly and inspection after multiple shut downs during the initial commissioning phase. The findings included rub damage to the expander wheel front seal and evidence of erosion damage at the inlet of the expander wheel blades (see Figure 8 and Figure 9). Another discovery was a discoloration at the bottom part of the expander casing area, which is exposed to inlet gas, suggesting liquid accumulation. The seal was cleaned and adjusted to increase the wheel-to-seal clearance, from .010" to .020" radially, with the goal of allowing any trapped liquids to more freely move through the seal. This was done by grinding out the seal and removing a spacer gasket from behind the seal (see Figure 4 and Figure 10).

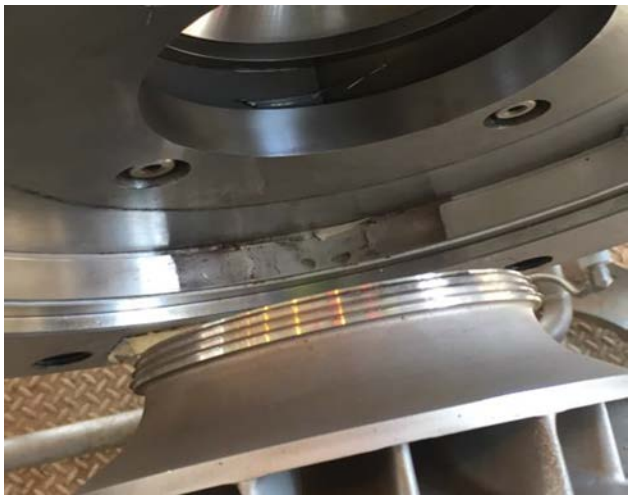

Figure 8. Picture of expander wheel and part of expander casing.

Figure 9. Evidence of erosion on suction surface of expander wheel.

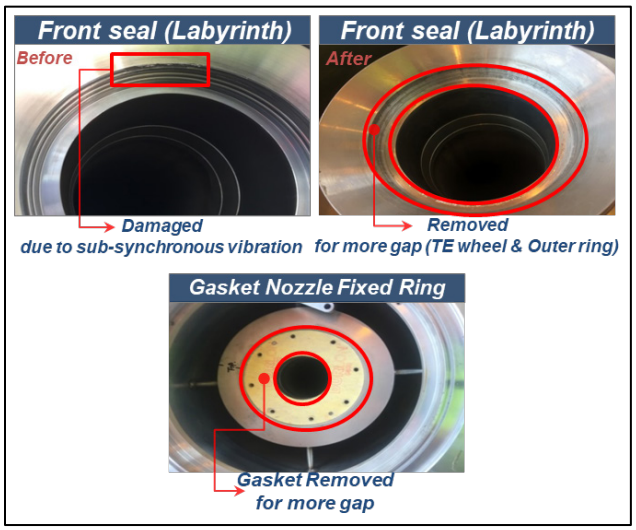

Figure 10. Modification of front seal to increase clearance.

Following the inspection and front seal modification, the machine was re-assembled and re-tested late August 2017. Different ramp-up rates were attempted to no avail. The machine was stable only for a short period of time before it would trip on high sub-synchronous vibration (see Figure 11 for waterfall plot). The increase in the front seal clearance did not lead to an improvement in operation, which lessened the credibility of the liquid-entrapment hypothesis.

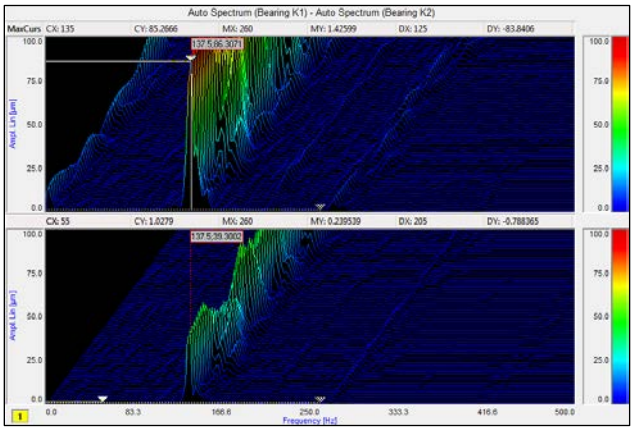

Figure 11. Spectrum analysis of high sub-synchronous vibration, tripping at ~137 Hz vibration frequency while running at ~15,600 RPM (260 Hz).

Over the subsequent months, the EPC made a tremendous effort to ensure dry gas was supplied to the expander inlet. Heat tracing and insulation were added, and the inlet separator design and sizing were revisited (see Figure 12). Other attempts were made to ameliorate the situation, namely, the level setpoint of the inlet separator was reduced.

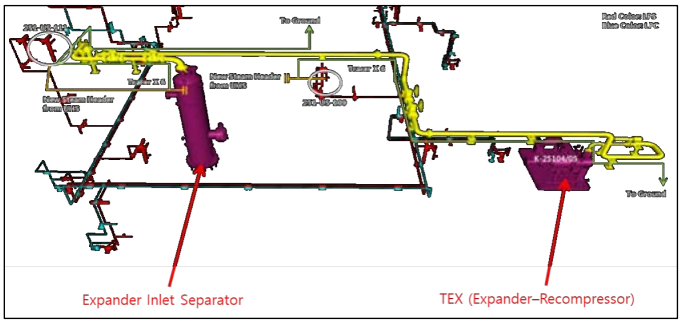

Figure 12. Plant 3D model showing section of piping heat traced.

Various operational improvements brought the process conditions closer to design conditions, specifically the pressure ratio across the expander wheel. The expander discharge and compressor suction pressure were reduced to about 290 psia with expander inlet pressure of about 1100 psia, much closer to the design operating cases. Despite all these changes and further trial runs, the machine tripped again due to high sub-synchronous vibration, this time at ~21,500 rpm.

The AMB supplier tried to maximize the stiffness and damping of the AMBs by modifying the AMB controller. Refer to Figure

13 for a comparison of the original and revised AMB controller transfer functions for the expander side bearing. The increase in gain provides more stiffness and additional phase lead angle tends to provide more rigid body damping. With these controller modifications, the unit was able to reach ~25,000 rpm, before tripping again due to high sub-synchronous vibration. This was the highest speed since the start of the commissioning effort, but the unit was still not processing full design capacity.

By late November 2017, all parties agreed that further investigation into the gas composition and phase(s) of the expander inlet stream held little potential to resolve the issue. All avenues relating to the AMBs that could possibly contribute to resolution of the sub-synchronous vibration problem appeared to have been exhausted. Clearly the speed at which the TEX became unstable varied with both process conditions and AMB controller changes, so a review of rotordynamics became necessary.

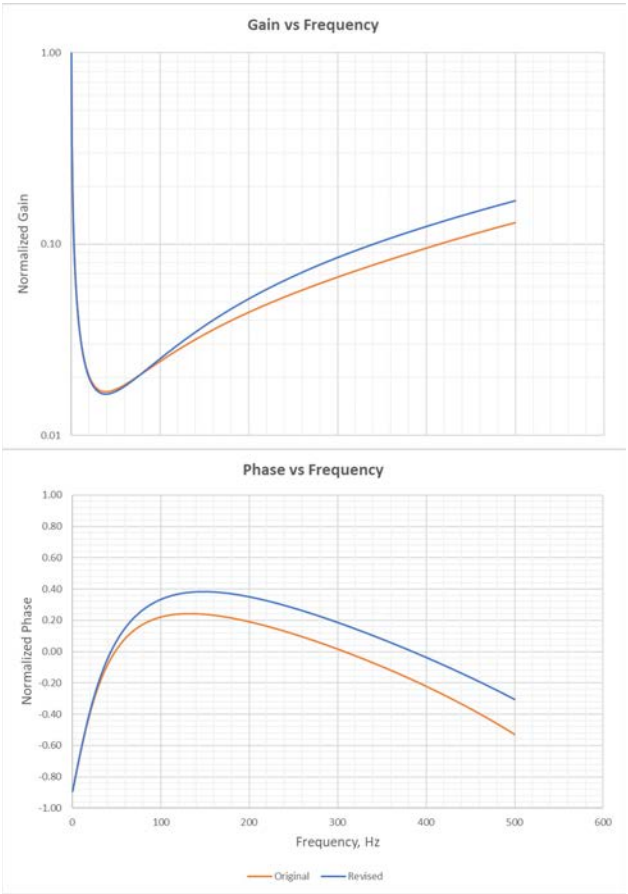

Figure 13. Comparison of original and revised AMB Controller transfer functions.

Rotordynamics Analysis

The TEX was designed according to the requirements of API-617, Seventh Edition. Section 2.6.5, which pertains to Level 1 stability analyses, states that "A stability analysis shall be performed on all centrifugal or axial compressors and/or radial flow rotors except those rotors whose maximum continuous speed is below the first critical speed in accordance with 2.6.2.3, as calculated on rigid supports…" Annex 4F of API-617, Seventh Edition, does not contain any additional analysis requirements. The aspect ratio (L/D) of a TEX shaft is usually small. As a result, the first bending mode of a TEX is almost always greater than the maximum continuous speed (MCS) of the machine. Therefore, a literal interpretation of paragraph 2.6.5.1 from API-617, Seventh Edition suggested that a Level 1 stability analysis was not necessary for this TEX.

For machines supported on oil bearings, this is usually an adequate approach since the bearings provide a high level of damping for the first two rigid body modes (i.e. translation and conical), and generally provide substantial separation margin from instability. However, AMB equipped machines may be susceptible to instability of the rigid body modes, if significant destabilizing cross-coupling effects are not fully addressed during the design of the AMB control algorithm. The typical stiffness for the AMB normally results in two rigid body modes being located within the operating speed range, so quantification of any cross-coupling effects is important to evaluate stability.

There are limited options available to the OEM and/or End User to retrofit an AMB-equipped TEX in order to resolve a sub-synchronous vibration issue. The common solutions afforded by oil bearings, such as changes in clearances, addition of squeeze film dampers, or an increase in oil viscosity to increase damping are unavailable. In addition, AMBs can be limited as to how much stiffness and damping they can provide. These include material limits on magnetic flux density, thermal limits within the coils and actuators, and amplifier current limits, among others. See a detailed discussion on these limitations in Swanson, 2014. In the subject machine, the efforts to maximize the capability of the bearing system had proved insufficient. Thus, the only recourse left was to reduce the cross-coupling effects by means of an invasive re-design.

The first step in this effort was to revisit the machine's rotordynamic analysis in order to determine whether it was possible for cross-coupled forces to be large enough to reduce the onset speed of instability so dramatically. Cross-coupled stiffness coefficients (i.e. $K_{xy} = -K_{yx}$) produce a tangential force normal to the rotor deflection direction. Supposing $K_{xy} > 0$ and $K_{yx} < 0$, if the rotor is perturbed in the positive X-direction, the cross-coupled stiffness coefficients lead to a force in the positive Y-direction. Now that the rotor has been perturbed in the positive Y-direction, it is forced in the negative X-direction. This leads to unstable, self-excited vibration.

The aerodynamic cross-coupling stiffness coefficient for the expander wheel was modeled using the API-Wachel equation as follows:

$$k_{xy} = 63{,}000 \frac{B \cdot HP}{RPM \cdot D \cdot h} \left(\frac{\rho_i}{\rho_o}\right)$$

Where:

k_{xy} = cross-coupling for wheel (lbf/inch)
B = 3
HP = power
D = diameter (inches)
h = minimum flow passage width (inches)
(ρ_i/ρ_o) = ratio of inlet to outlet density

Note that the density ratio was inverted in order to maintain a ratio higher than one, since this is a radial flow turbine whereas the equation is originally expressed for a centrifugal compressor. The labyrinth seal rotordynamic coefficients were modeled using a commercially available code, which is based on a 1D isothermal control volume model (Figure 14 shows the rotordynamic model.) Figure 15 depicts the rotordynamic stability results in the form of a damping factor map. With the API-Wachel and labyrinth seal cross-coupled effects applied, the analysis predicts stable operation at all speeds of interest, from 0 up to 40,000 rpm. Note that API-Wachel and labyrinth seal cross-coupled effects were not included for the compressor wheel because both were over an order of magnitude lower than the respective values of the expander wheel.

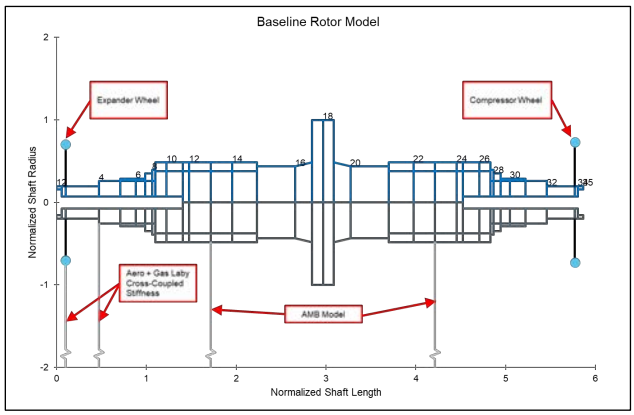

Figure 14. Baseline rotordynamic model.

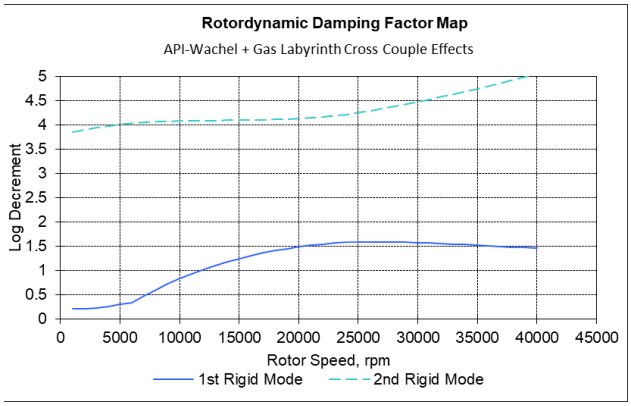

Figure 15. Baseline design damping factor map.

The model was modified by adding a single cross-coupled stiffness value located at the rear of the expander wheel to represent a "lumped" stiffness that included the combined effects of the wheel and the seals (see Figure 16). The magnitude of this "lumped" cross-coupled stiffness was "tuned" to vary as a function of speed such that the model's predictions would match the onset speed of instability observed in the field. The result of this simulation is shown in Figure 17, which shows the onset of instability of the 2nd rigid body mode around 25,000 rpm. Figure 18 shows the mode shape of the unstable mode, which was consistent with the vibration observed at site, namely conical rigid body motion.

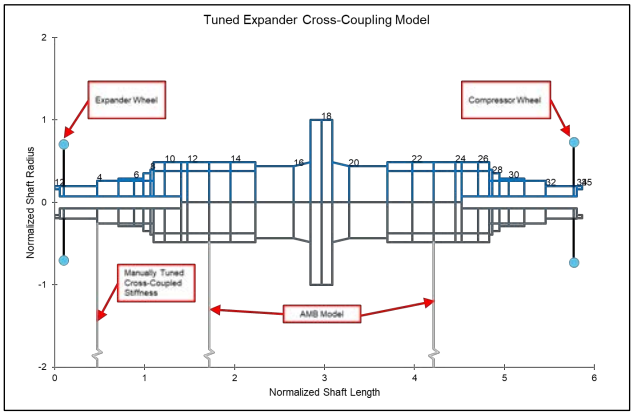

Figure 16. Modified rotordynamic model showing "tuned" Kxy value at the expander wheel location.

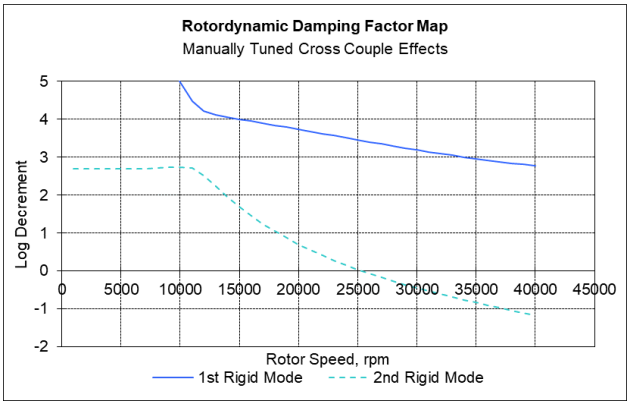

Figure 17. Damping factor map of tuned model, showing onset speed of instability at ~25000 rpm.

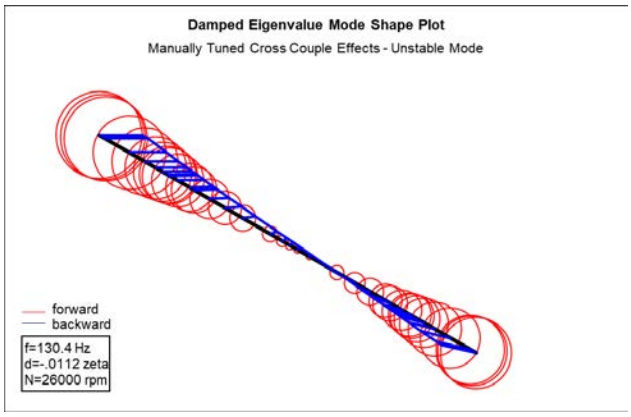

Figure 18. Mode shape of unstable mode.

Figure 19 shows that the "tuned" Kxy value was almost 6 times higher than the API-Wachel equation, underscoring some of the current limitations that exist to account for cross-coupling in the design of radial inflow expander wheels. These results support the recommendation of API-617 of checking for Kxy up to 10 times API-Wachel. However, there is still much uncertainty in this approach for the designer. The API-Wachel formula is based on an empirical derivation (Evans, 2010) and the 10X is essentially a rule-of-thumb. To date there is no reliable method for accurately estimating the contribution of the aerodynamic coupling in a radial inflow turbine wheel. Besides, there are no analysis codes currently available that model two-phase flow in a labyrinth seal.

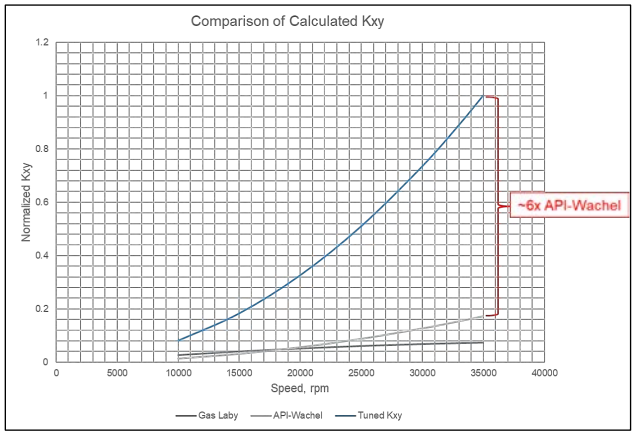

Figure 19. Comparison of tuned Kxy vs. existing equations.

To appreciate the challenges involved in the rotordynamics of this machine, it is necessary to acknowledge that both aerodynamic and labyrinth seal cross-coupled effects are largely dependent on the following aerodynamic parameters and fluid properties:

1. Gas swirl ratio (SR), commonly defined as the tangential velocity of the gas divided by an appropriate surface speed (e.g. wheel tip, or labyrinth seal)

2. Gas density around the periphery of the wheel and seals, which is a function of pressure, temperature and molecular weight

3. Overall machine pressure ratio

4. Wheel seal clearances

Of these, the designer has direct, but limited, control of swirl ratio and density around the wheel periphery, as well as wheel seal clearances. The available literature on the topic of cross-coupled loads on rotors is primarily centered around compressors. Various studies suggest a strong dependency on SR. It is suggested that as SR approaches unity, the gas can induce destabilizing cross-coupled loads on the impeller, leading to rotordynamic instabilities. The same principle applies to fluids swirling in labyrinth seals (Baldassarre, 2014). These studies suggest various solutions for such phenomena, all centered around reducing swirl velocity. However, compressor swirl ratios are typically low relative to expanders. As discussed in API-684, Second Edition, common "fixes" include installation of swirl brakes and shunt lines, and replacement of labyrinth seals with pocket damper, honeycomb, or hole pattern seals, in order to reduce swirl velocity and add direct damping. TEX swirl ratios are nominally on the order of one or higher for a "good" design (i.e. optimum efficiency). High swirl is a desirable characteristic in a TEX and a necessary condition for effective performance. Hence, attempts to reduce swirl should be weighed carefully, because of the adverse effect in the performance of the TEX. Similarly, design wheel seal clearances should be as tight as possible to maximize efficiency. However, tight seal clearances directly contribute to destabilizing labyrinth seal cross-coupled effects. It should be apparent that a well-designed TEX will inevitably have high cross-coupled stiffness effects! Therefore, the goal is to design a rotor-bearing system that can handle these high loads.

One can consider unstable vibration as a continuous addition of energy into the rotor that cannot be removed by a damping mechanism in the bearing system. This energy must come from the gas stream, in essence a momentum transfer from the gas to the rotor. Therefore, in the opinion of the authors, a valuable figure of merit to consider is a product of gas density and swirl velocity. Specifically, a figure proportional to gas momentum (i.e. $\sim\rho V^2$) times the blade width (b) can serve as a criterion for the assessment of potentially high cross-coupled aerodynamic effects. Table 3 below summarizes the recent experience of this OEM. The table is sorted by this figure of merit ($\rho V^2 b$) from high to low. Incidentally, it was discovered that both the N'Kossa machine (Job 1) and this machine (Job 3) were on the high side of the range of $\rho V^2 b$.

A detailed CFD study (Lerche, 2013) attempted to analytically quantify aerodynamic cross-coupled loads in an expander application. In this study, the authors approach the problem by performing a transient CFD study of an expander stage with the expander wheel slightly eccentric with respect to the guide

vanes' centerline. An average cross-coupled stiffness was then derived by dividing the resultant radial load computed by the CFD solver by the amount of eccentricity imposed perpendicular to the load vector. The resulting value for the design and operating case studied suggested a load that is less than that predicted by the API-Wachel equation. The study references another equation, called the SwRI-Wachel equation, which is derived from a CFD study by Moore, 2011, as follows:

$$k_{xy} = C_{mr}\rho_d U^2 L_{shr}\left(\frac{Q_{design}}{Q}\right)$$

Where:

k_{xy} = cross-coupling for the wheel
C_{mr} = dimensionless cross-coupled coefficient
ρ_d = discharge density
U^2 = square of wheel tip speed
L_{shr} = minimum flow passage width
(Q_{design}/Q) = relative flow

Though derived for a compressor application, note the dependence on ρU^2 as opposed to power and speed (i.e. torque) as in the API-Wachel equation. The cross-coupled stiffness derived using this SwRI-Wachel equation is approximately 3.4 times higher than the API-Wachel value, and in this OEM's opinion is a better starting point.

Another parameter of interest is torque. The international standard ISO 14839 suggests the radial loads imposed by impellers is a percentage of the torque. It states, in Part 4, Para. 8.1.1, that "the conditions of a fluid static load are defined by assuming that the side load equivalent to 4% of all the fluid torque at normal operation affects the outer diameter of each impeller." In the case of this machine, the 4% recommendation did not appear to cause instability in the initial rotordynamic analysis. In addition, Table 3 shows that there are projects with higher magnitudes of torque of the same frame size and AMB configuration as the subject machine that are stable, suggesting using torque as a criteria alone is insufficient.

The most important parameters appear to be inlet pressure, pressure ratio and molecular weight, as they directly affect the $\rho V^2 b$ figure of merit. The authors recommend that a review of these parameters within the OEM and AMB supplier's references be carefully considered as early as possible in the design process. Of course, these comparisons should be between machines of comparable frame size and rotor/bearing layout.

In summary, the current tools for predicting cross-coupling loads need to be improved and more research is necessary to fully understand the phenomenon and formulate effective preventive solutions.

API-617, Eighth Edition, takes a more conservative approach to stability analysis of AMB equipped turbomachinery. In Chapter 1, Annex E, paragraph E.4.8.5.1, it states that "A Level I stability analysis as described in 4.8.5 shall be performed on all AMB supported compressors…." The experience of the authors suggests this is a much more appropriate design and analysis approach to ensuring stable operation of AMB equipped turboexpanders.

Table 3. Comparison of various figures of merit from recent projects.

Job	Type	MW	Pr	ρ [lb/ft3]	V swirl [ft/s]	U [ft/s]	SR	b [in]	$\rho V^2 b$ [lb/in]	Speed [rpm]	Power [hp]	Torque [ft-lb]	Wachel [lb/in]	Est. Disch. Liq. %
1 N'Kossa	AMB	20.3	3.0	4.21	786	874	0.9	1.79	**1003**	21,300	5824	1436	5339	15.3
2	Oil	19.2	4.2	2.94	1032	909	1.1	1.25	**845**	24,500	2470	529	3334	20.4
3 This Paper	AMB	23.8	4.1	3.76	978	982	1.0	1.03	**804**	30,000	2206	386	3677	27.7
4 Re-design	AMB	23.8	4.1	4.32	871	969	0.9	1.03	**733**	29,600	2129	378	4154	23.8
5	AMB	18.6	3.0	3.09	908	853	1.1	1.30	**716**	23,000	2806	641	3411	13.2
6	Oil	18.4	3.0	2.90	887	804	1.1	1.30	**643**	21,682	2231	540	2599	16.1
7	AMB	18.9	2.6	2.50	877	779	1.1	1.44	**599**	21,000	2064	516	2261	13.0
8	AMB	17.5	2.5	3.04	806	834	0.9	1.31	**558**	22,500	2990	698	3606	8.0
9	AMB	18.6	1.3	5.64	420	467	0.9	1.35	**290**	13,800	1115	424	1547	0.8
10	AMB	4.5	1.3	0.51	1024	1032	1.0	1.10	**127**	43,000	382	47	311	6.4
11	AMB	8.6	2.3	0.96	781	868	0.9	0.98	**125**	25,270	350	73	457	9.2
12	AMB	4.3	1.3	0.38	1041	1032	1.0	1.28	**115**	43,000	367	45	258	6.7
13	AMB	8.1	2.3	0.43	748	831	0.9	1.30	**68**	22,400	290	68	301	7.2

Decision to consider a redesign – November 2017

The OEM and EPC agreed to redesign with the explicit intent to minimize liquid formation after the inlet guide vanes, minimize swirl velocity, and add damping at seal locations.

The redesign strategy of the expander wheel was deliberated at length. The OEM maintained that a shrouded wheel was necessary for structural (i.e. resonance) reasons. By reducing the discharge flow area, and therefore the pressure at the inlet of the wheel, the blade loading was increased substantially. In addition, not much margin would be left against a choked condition for higher flow off-design cases. The improvements, if any, brought about by a shroudless (open) wheel could not outweigh the risks of a structural failure. The research in the preceding months suggested that high density and high swirl velocity were the key contributors for cross-coupling effects. The issue being that the amount of liquid leads to an increase in density, not that presence of liquid phase is a problem in and of itself. As explained earlier, all TEXs operating in a natural gas application with saturated gas at the inlet will have liquid produced through the guide vanes. Therefore, in the opinion of the OEM, increasing the pressure at the wheel outer diameter would have the largest benefit (i.e. reduction in cross-coupled stiffness), and a shrouded wheel would maximize this benefit. However, the EPC was rightfully concerned about liquid related issues. After all, the N'Kossa case history suggested that TEX's operating in high liquid content conditions should use open wheels, so that there is no possibility of trapping condensed liquids in the periphery of a shrouded wheel. A shrouded wheel was chosen out of necessity to avoid structural failure due to resonance.

Figure 20 and Figure 21 compare computational fluid dynamics (CFD) results of the original and redesigned expander wheels in a blade-to-blade plot. An important take away is the reddish areas around the blade discharge of Figure 21, indicating high Mach number and the onset of choked flow. This is not a well-designed expander wheel if optimum efficiency is desired, however efficiency had to be sacrificed to reduce swirl velocity.

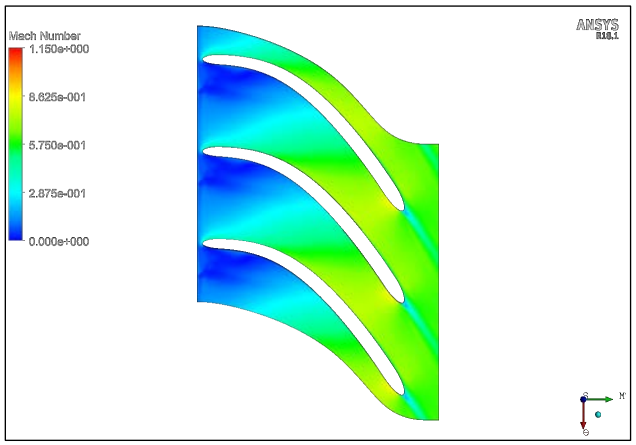

Figure 20. CFD analysis results of the original design, showing relative Mach number at 50% of blade height.

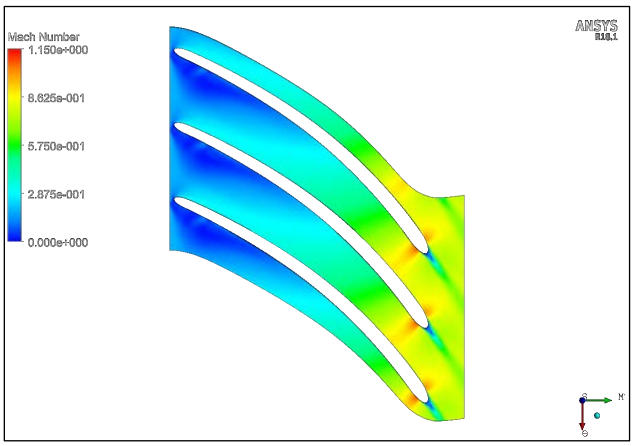

Figure 21. CFD analysis results of the redesign, showing relative Mach number at 50% of blade height.

The OEM predicted that the redesigned expander wheel would increase wheel inlet pressure by ~20%, increase wheel inlet density by ~15%, reduce liquid content by ~14%, and most importantly reduce swirl velocity by ~13%. The net effect was approximately a 10% reduction in the $\rho V^2 b$ figure of merit.

Figure 22 shows a picture of the finished front wheel seals with swirl brakes. Figure 23 shows a section view of the rear pocket damper seal highlighting the fully partitioned pocket damper seal, the swirl brakes, and the holes provided as provisions for gas injection. The primary reason for choosing a pocket damper seal design was for an increase in direct damping coefficient, as well as a reduction in cross-coupled stiffness. This type of seal operates at an increased clearance and suffers from increased seal leakage. It was difficult to estimate the negative impact on expander stage efficiency because there are no analysis codes currently available that model two-phase flow in a labyrinth or pocket damper seal. The stiffness and damping coefficients estimated from the pocket damper seal manufacturer were based on gas-only models. Nevertheless, quantitatively speaking there was confidence that the pocket damper seal design would provide significantly more damping than a labyrinth seal. In addition, the process designers were confident a reduction in expander efficiency would not jeopardize the overall plant production requirements and was therefore worth the risk.

Figure 22. Redesigned front wheel seals.

Figure 24 compares the Log Dec curves from rotordynamic analysis of the original design with tuned cross-coupled stiffness (Figure 17) and the same model including the estimated damping from the PDS. Note that this analysis did not consider the fact that the redesigned expander wheel should have also reduced the magnitude of cross-coupled stiffness. Therefore, the analysis suggested that the PDS type seals alone had the potential to fully alleviate the sub-synchronous vibration issue. Absent schedule and cost restrictions the authors would have preferred to simply install the pocket damper type seals with the existing wheel design. Unfortunately, when faced with a troubling machine, all possible remedies must be incorporated at once.

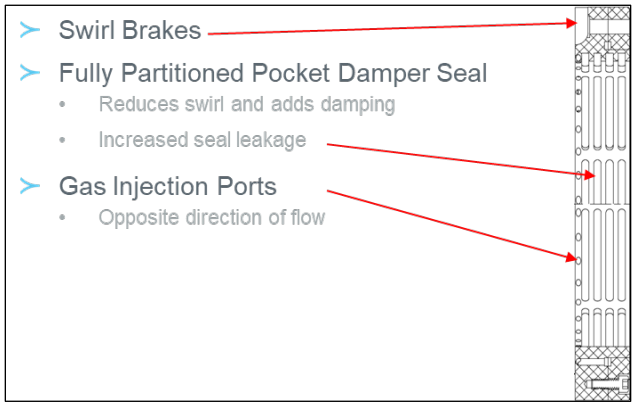

Figure 23. Summary of pocket damper seal design.

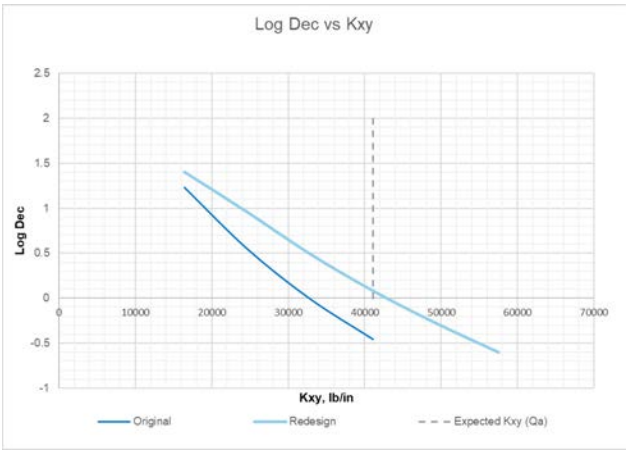

Figure 24. Comparison of original and redesigned Log Dec curves.

RESULTS OF REDESIGN

The redesigned expander wheel and seals improved rotordynamic stability and achieved close to design performance. Below is a summary of the redesign features along with their intended effects (also refer to Figure 25).

1. Expander wheel with reduced discharge flow area, which maximized the pressure at the outer diameter of the expander wheel to reduce swirl velocity.

2. Pocket Damper seals with integral swirl brakes, which minimized swirl velocity, reduced cross-coupled stiffness, and added direct damping.

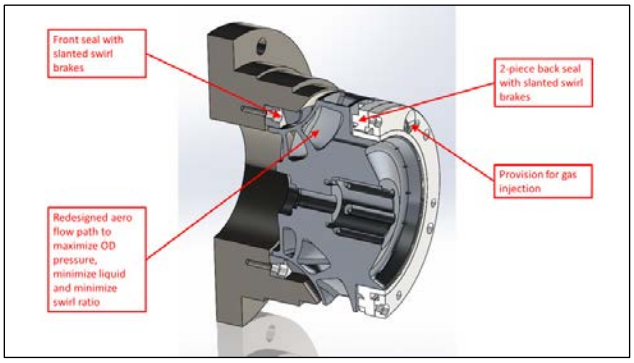

Figure 25. Summary of redesign features.

As a result of these modifications, the TEX was able to operate at full plant capacity with negligible vibration levels (see Figure 26). Table 4 lists pertinent performance data from site, compared to original design conditions.

Table 4. Performance date after redesign.

	Site – 3/12/2018		Original Design	
	Exp	**Comp**	**Exp**	**Comp**
MW	21.17	20.31	23.82	20.82
Pin [psia]	1176	258	1165	247
Tin [F]	84	95	86	99
Flow [lb/hr]	157,000	125,000	160,000	121,000
Pout [psia]	277	422	286	450
Tout [F]	-7	169	-9	195
Speed [rpm]	26,500		30,000	

Though the machine did not reach the original design speed of 30,000 rpm, the results were found acceptable by the EPC and End User because the overall plant performance achieved design targets. The plant was able to process the required capacity and the TEX discharge temperature was below process requirements as well, indicating the overall efficiency was acceptable.

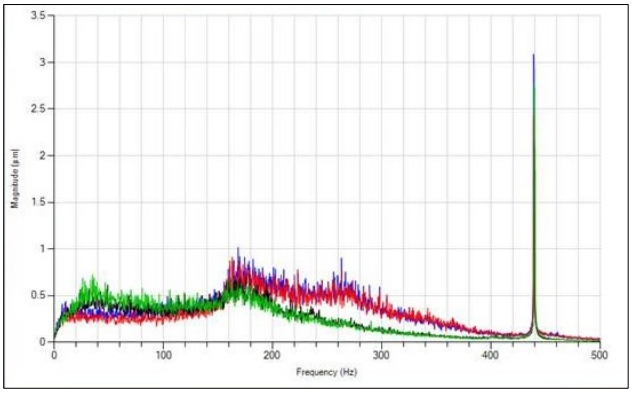

Figure 26. Spectrum analysis of redesigned unit operating at about 25,000 rpm (420 Hz), with negligible sub-synchronous vibration.

The expander molecular weight and mass flow rate had decreased, leading to a reduced expander output versus design, and the mass flow rate through the compressor had increased, leading to an increased load versus design. Combined with an expected reduction of expander efficiency, the lower speed did not come as a surprise.

CONCLUSIONS

Large aerodynamic forces acting upon a radial inflow TEX wheel are to be expected in many designs and operational conditions. These forces introduce cross-coupling effects to the rotor-bearing system, which in some cases, precipitate crippling vibrational instabilities. Oil bearings generally have more margin to counteract these forces, while magnetic bearing machines require more extensive analysis and design practices to ensure the cross-coupled forces will not cause instability. The case study described in this paper illustrates the extent of analysis procedures and design practices that may be required for an AMB machine.

Upon initial commissioning, the subject machine was not able to achieve operating speed, failing to achieve performance requirements. After field troubleshooting and rotordynamic simulations, it was determined that the best explanation was that the aerodynamic and labyrinth seal induced cross-coupled forces were higher than the stabilizing capabilities of the AMB system available for this project. This experience showed that these forces are poorly understood for the TEX designers due to a lack of analytical tools and experimental data. Currently designers must rely on empirical relationships (e.g. API-Wachel formula) and rules of thumb (e.g. the 10X API-Wachel) to predict these forces. The experience presented in this paper confirms that it is a highly recommended practice to perform a Level 1/2 stability analysis and at minimum to use 10 times the API-Wachel value for the rotordynamics model for all AMB equipped TEXs. Furthermore, a figure of merit ($\rho V^2 b$) is suggested as a valuable guiding parameter for comparing with successful reference projects.

The machine described in this paper was retrofitted via the following: 1) an expander wheel re-design (to reduce swirl velocity), 2) addition of pocket damper seals to the front and back seals of the expander wheel to add damping to the rotor-bearing system, and 3) swirl breakers integrated in the wheel seals. These modifications effectively corrected the issue and allowed the machine to reach desired performance.

More End Users, particularly those in the U.S. natural gas industries, are beginning to embrace the many operational advantages that AMBs offer over their oil-bearing counterparts. The experience described herein underlines the need for research efforts in the area of aerodynamic loading on radial inflow expanders to ensure robust designs are developed.

Furthermore, the ability of AMBs to introduce programmable in-situ force excitations and real-time load and displacement measurements may prove effective in providing experimental data. These will serve to better understand the phenomena at play and to undergird future analytical efforts, such as CFD for stator-to-rotor interaction.

REFERENCES

API 617, 2002, "Axial and Centrifugal Compressors and Expander-Compressors for Petroleum, Chemical and Gas Industry Services," Seventh Edition, American Petroleum Institute, Washington, D.C.

API 617, 2014, "Axial and Centrifugal Compressors and Expander-Compressors for Petroleum, Chemical and Gas Industry Services," Eighth Edition, American Petroleum Institute, Washington, D.C.

API 684, 2005, "Tutorial on Rotordynamics: Lateral Critical, Unbalance Response, Stability, Train Torsional and Rotor Balancing," Second Edition, American Petroleum Institute, Washington, D.C.

Baldassarre, L.; Guglielmo, A.; Bernocchi, A.; Masi, G.; Fontana, M., 2014, "Optimization of Swirl Brake Design and Assessment of Its Stabilizing Effect on Compressor Rotordynamic Performance." *Proceedings of the 43rd Turbomachinery Symposium*.

Evans, B.; Fulton, J.; 2010, "Wachel's Equation – Origin and Current Evaluation of API-617 Rotor Stability Criteria." *Proceedings of the 39th Turbomachinery Symposium.*

Jumonville, Jigger, 2010, "Tutorial on Cryogenic Turboexpanders." *Proceedings of the 39th Turbomachinery Symposium.*

Lerche, A.; Musgrove, G.; Moore, J.; Kulhanek, C., 2013, "Rotordynamic Force Prediction of an Unshrouded Radial Inflow Turbine Using Computational Fluid Dynamics." *Proceedings of ASME Turbo Expo 2013: Turbine Technical Conference and Exposition.*

Lillard, J.; Nordwall, G.; Elliott, G.; Shoup, T.; Moore, J.; Kulhanek, C., 2017, "Eliminating a Rotordynamic Instability of a 12 MW Overhung, Radial Inflow Expander." *Proceedings of the 46th Turbomachinery Symposium*.

Moore, J.; Ransom, D.; Viana, F., 2011, "Rotordynamic Force Prediction of Centrifugal Impellers Using Computational Fluid Dynamics," *Journal of Engineering for Gas Turbines and Power.*

Shokraneh, H.; Richaume, L.; Quoix, B.; and Oliva, M., 2016, "Sub-synchronous Vibrations on Turboexpanders Equipped With Magnetic Bearings: Assessment, Understanding and Solutions." *Proceedings of the 45th Turbomachinery Symposium.*

Swanson, E.; Hawkins, H.; Masala, A., 2014, "New Active Magnetic Bearing Requirements for Compressors in API-617 Eighth Edition." *Proceedings of the 43rd Turbomachinery Symposium.*

ACKNOWLEDGMENTS

The first and second authors would like to thank Eric Gentilini, Todd Heninger, Chasen Murphy and the rest of the shop, engineering and sales teams at L.A. Turbine as well as the team at SKF/S2M Magnetic Bearings for their expertise and dedication to this project. The authors would also like to acknowledge the contributions of the following individuals: Dr. Dara Childs for his helpful insight into the rotordynamic issues and redesign effort, Brian Parrelli for his work on the aero redesign of the expander wheel, Dr. Thomas Chirathadam and Bearings Plus Inc. for the fast turnaround on the design and manufacture of the pocket damper seals, Richard Shultz for his valuable advice throughout the troubleshooting process, and Dr. Brian Murphy and Dan Lubell for their helpful advice with the rotordynamics modeling. The third author would also like to thank GPNB and the CPF Phase II project team at Badra Oil Field, Iraq, and the Samsung Engineering home office and site support team.